UNIVERSITY OF BIRMINGHAM
University of Birmingham Research at Birmingham

Fracture trace length and number distributions from fracture mapping

Riley, Michael

DOI:
10.1029/2004JB003164

Document Version
Publisher's PDF, also known as Version of record

Citation for published version (Harvard):
Riley, M 2005, 'Fracture trace length and number distributions from fracture mapping', *Journal of Geophysical Research*, vol. 110, pp. B08414. https://doi.org/10.1029/2004JB003164

Link to publication on Research at Birmingham portal

Publisher Rights Statement:
Riley, Michael S., (2005), Fracture trace length and number distributions from fracture mapping, Journal of Geophysical Research, vol. 110, DOI 10.1029/2004JB003164. To view the published open abstract, go to http://dx.doi.org and enter the DOI. An edited version of this paper was published by AGU. Copyright (2005) American Geophysical Union.

General rights
Unless a licence is specified above, all rights (including copyright and moral rights) in this document are retained by the authors and/or the copyright holders. The express permission of the copyright holder must be obtained for any use of this material other than for purposes permitted by law.

•Users may freely distribute the URL that is used to identify this publication.
•Users may download and/or print one copy of the publication from the University of Birmingham research portal for the purpose of private study or non-commercial research.
•User may use extracts from the document in line with the concept of 'fair dealing' under the Copyright, Designs and Patents Act 1988 (?)
•Users may not further distribute the material nor use it for the purposes of commercial gain.

Where a licence is displayed above, please note the terms and conditions of the licence govern your use of this document.

When citing, please reference the published version.

Take down policy
While the University of Birmingham exercises care and attention in making items available there are rare occasions when an item has been uploaded in error or has been deemed to be commercially or otherwise sensitive.

If you believe that this is the case for this document, please contact UBIRA@lists.bham.ac.uk providing details and we will remove access to the work immediately and investigate.

Download date: 04. May. 2023

Fracture trace length and number distributions from fracture mapping

Michael S. Riley

Hydrogeology Research Group, Earth Sciences, School of Geography, Earth and Environmental Sciences, University of Birmingham, Birmingham, UK

Received 5 May 2004; revised 13 April 2005; accepted 18 April 2005; published 31 August 2005.

[1] Statistical distributions of fracture trace length and density determined from two-dimensional fracture mapping generally provide biased estimates of the underlying distributions due in part to edge effects of the finite window of observation (censoring) and the protocol adopted for recording short traces (lower truncation limit). Although methods for estimating the parameters of an assumed underlying distribution exist, validation of the inferred models by forward prediction of the observed length distribution is rarely undertaken since mathematical formulations of the required distributions are not reported in the literature. This paper presents formulae that can be used simply to obtain these distributions, with results for rectangular windows given as a specific example. Formulae relating the observed and underlying fracture density are also given. The formulae are presented for underlying trace lengths that can be characterized by exponential, lognormal, or finite range power law distributions. Results for the semi-infinite range power law can also be obtained simply. The formulae are based upon the assumption that fracture locations can be adequately described by a uniform Poisson process, although the methodology is described more generally. The distributions of uncensored, singly censored and doubly censored trace lengths are also derived. The effects of the window of observation and the lower truncation limit for the frequently assumed semi-infinite range power law are outlined.

Citation: Riley, M. S. (2005), Fracture trace length and number distributions from fracture mapping, *J. Geophys. Res.*, *110*, B08414, doi:10.1029/2004JB003164.

1. Introduction

[2] Stochastic models of flow and transport in fractured rock, used regularly in hydrogeological, nuclear waste disposal, geotechnical, and oil reservoir investigations, are based upon statistics, gathered from field surveys, that describe fracture size and density. One of the field techniques from which statistics can be inferred is the complete mapping of one or more outcrops, usually in two dimensions. Many studies acknowledge that there are biases inherent in using the results of such surveys to estimate fracture density and the underlying distribution of fracture trace length, but comparatively few attempt to quantify and correct for them. The importance of understanding the nature and size of these biases is commonly acknowledged [e.g., *Bonnet et al.*, 2001; *Berkowitz*, 2002; *Jing*, 2003]. *Pickering et al.* [1995] give a summary of the principal biases. The sources of bias fall into two categories: those that are purely statistical in nature, and which can be accounted for mathematically; and those that require the application of geological models and expertise to resolve. The statistical biases are due to edge effects relating to the finite window of observation, and the use of a minimum recordable trace length in well-conducted fieldwork. These are commonly, although not universally, referred to as censoring and (lower or left hand) truncation, respectively.

[3] The method for analyzing the biases in fracture size and density depends upon the structure of the rock under investigation. In thin bedded, sedimentary sequences such as those described by *Lloyd et al.* [1996] and *Pascal et al.* [1997], the subvertical fracturing in a particular layer can be well described by a two-dimensional model in which fracture size is characterized by trace length. In contrast, three-dimensional models of fracture size are necessary in granitic formations, although in practice, such models are often constructed from a number of two-dimensional sections. This paper deals solely with the two-dimensional case.

[4] If the statistics from field data are to be used in stochastic simulations, an underlying distribution of fracture trace lengths has to be established and its parameters estimated. *Bonnet et al.* [2001] note that partly due to the problem of analyzing biases in sampling, it is common for a power law distribution to be assumed a priori. To make a rational choice between candidate distributions, a method of comparing their goodness of fit to a data set that takes sampling biases into account needs to be established.

[5] There is an extensive literature on the problem of estimating the parameters of the underlying fracture length

Copyright 2005 by the American Geophysical Union.
0148-0227/05/2004JB003164$09.00

distribution from field data collected in a finite window. Results derived for scan line investigations are also numerous, but are not considered here. Similarly, since the problem considered in this paper is essentially two-dimensional, discussion of stereological models is not included.

[6] Nonparametric estimation of mean trace length from observation data has been discussed by several authors. *Pahl* [1981] gives a result for parallel fractures in a window of constant height and infinite width. *Kulatilake and Wu* [1984] consider fractures with a known orientation distribution, observed in a rectangular window, and assume independence of fracture orientation and length. *Lindsay and Rothrock* [1995] and *Odling* [1997] apply the Kaplan-Meier estimator to leads in Arctic pack ice and fracture trace lengths, respectively. *Zhang and Einstein* [1998] deal with fracture traces observed in a circular window by considering the number of fracture traces that are uncensored, singly censored or doubly censored. Distribution free estimates of the mean are sometimes used to parameterize an assumed exponential distribution on the grounds that it is completely specified by its mean.

[7] Parametric methods of estimation require the a priori specification of the underlying distribution. Exponential, truncated exponential, and lognormal distributions were common in the early literature. The power law distribution with a semi-infinite range (i.e., a lower cutoff length, but no upper limit) has also been widely assumed. More recently, the finite range power law has received more attention [e.g., *Bour and Davy*, 1999; *Berkowitz*, 2002; *Harris et al.*, 2003]. Other possibilities include the Pareto class of distributions [*Clark et al.*, 1999], the Erlangian distribution [*White and Willis*, 2000], and the distribution described by *Riley* [2004]. In papers that remain the key works on the parameter estimation problem, *Laslett* [1982a, 1982b] describes maximum likelihood estimators for mapping and scan line survey data that account for edge effects for fractures with a known orientation distribution, and which are observed in a convex window of variable diameter. More recently, *Song and Lee* [2001] derived formulae for rectangular and circular windows relating the underlying distribution to the observed distributions of uncensored and singly censored traces. *Visser and Chessa* [2000] developed a method of correcting for edge effects by estimating the expected complete length of a partially exposed trace.

[8] Although parameters of a distribution can be estimated, the estimation process in itself does not generally validate the inferred model. Validation can be achieved by comparing the observed distribution with either a simulated distribution obtained by sampling the inferred distribution in a replica of the window of observation, or with a distribution derived theoretically. The first strategy is cumbersome, particularly when distributions with long tails, such as the lognormal or semi-infinite range power law, have to be simulated. The theoretical distributions required for the second approach are not reported in the literature.

[9] This paper presents the theoretical statistical distributions of trace length and density observed in a large class of sampling windows for a range of commonly assumed underlying fracture length distributions. Furthermore, the results are presented in a form that allows their use through the application of formulae. The methodology employed in deriving these formulae is also applicable to arbitrary distributions. The theoretical cdfs can be used directly in statistical inference simply by matching them directly with the empirical cdfs derived from field data using commonly available optimization software such as SOLVER within Microsoft EXCEL. However, the results presented here can be used most effectively to gain insights into the magnitude of the statistical biases involved in the sampling procedure, to validate inferred models, and hence to provide a sound basis for deciding between competing models of fracture length.

2. Fracture Maps in Directionally Nonreentrant Windows

[10] The following analysis explicitly accounts for the edge effects of a finite window of observation and the existence of a lower truncation limit, t_0, that is, the smallest trace length to be recorded in a particular survey. The lower truncation limit is a function of the method and scale of observation. The assumption made throughout is that all fractures in a set are parallel and straight. The analysis applies to convex windows, but also to a larger class of windows, described here as directionally nonreentrant. These are windows that cannot be intersected more than once by any fracture with a specified orientation. Figure 1a shows a schematic fracture map in an irregular window of observation. The window is nonreentrant in the direction of the north-south fractures but is reentrant relative to those with an east-west trend. Thus, although all north-south fractures can be described using the methods outlined in this paper, analysis of the second fracture set requires the data set to be restricted to those fractures contained in the window shown in Figure 1b.

[11] In the following, a directionally nonreentrant window is referenced by coordinate axes with the y direction parallel to the fracture set orientation and the x axis orientated so that points in the window have positive x coordinates (Figure 2). Any such window can be thought of as a collection of subwindows that are themselves directionally nonreentrant and whose width in the y direction (i.e., height), varies strictly monotonically or is constant. Figure 2 shows a compound window divided into three subwindows of width w_1, w_2, and w_3. The height of the subwindow, $i = 0$, 1, or 2, is $h_i(x)$. Since a fracture intersecting a window whose height is less than t_0 will not be recorded, the minimum height of the ith window, $h_i^{\min}$, is taken to be greater than or equal to t_0. The distance of the lower edge of the window from the x axis is $g_i(x)$. Figure 2 also shows an arbitrary fracture of length L intersecting subwindow 3.

[12] The approach adopted in the theoretical derivation of the observed trace length distributions is to partition any complex window into simple subwindows whose height varies strictly monotonically or is constant, to derive the distribution of trace lengths and number of fractures observed in each subwindow, and to use these to develop results for the entire window.

3. Observed Trace Length Distribution: General Case

[13] Let X and Y be the coordinates of the lower end of a randomly chosen fracture, which may or may not intersect a window, and let L be its length (Figure 2). Define T to be the

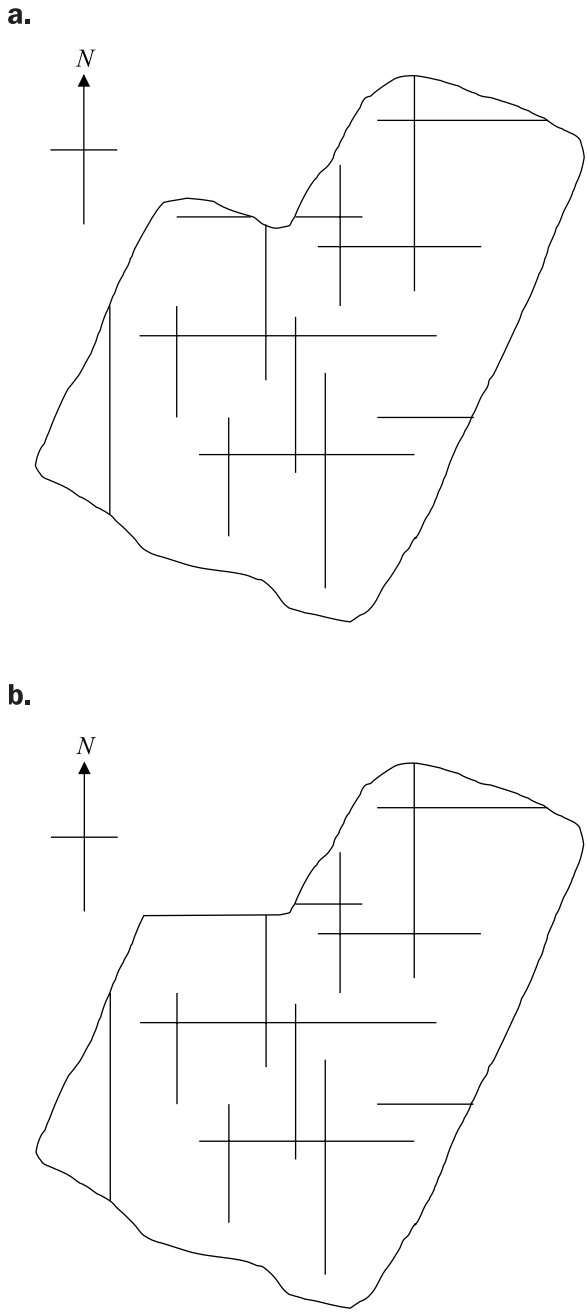

Figure 1. (a) Schematic fracture map in an irregular window of observation. (b) Window of observation, modified to be nonreentrant parallel to the east-west fractures.

actual trace length of the fracture within the window. The fracture will be observed (recorded) if the length of the trace in the window is greater than t_0. Let T^{obs} be the length of the fracture trace observed in the window. Then the cdf of T^{obs} is given by

$$\begin{aligned} P(T^{\text{obs}} < t) &= P(T < t | \text{trace is observed}) \\ &= \frac{P(T < t \text{ and trace is observed})}{P(\text{trace is observed})} \\ &= \frac{P(t_0 \le T < t)}{P(t_0 \le T)} \end{aligned} \tag{1}$$

which can be calculated by

$$P(T^{\text{obs}} < t) = \iiint_{t_0 \le T < t} k(\mathbf{s})\mathrm{d}\mathbf{s} \Big/ \iiint_{t_0 \le T} k(\mathbf{s})\mathrm{d}\mathbf{s} \tag{2}$$

where $k(\mathbf{s})$ is the joint pdf of X, Y, and L, and $\mathbf{s}$ is the triple (x, y, l).

[14] Equation (2) is applied first to a simple window and separately to traces that are uncensored, or censored once by either of the window edges (singly censored), or censored by two edges (doubly censored). The results are combined to give the cdf of the length of all traces observed in the window. The results for the simple window are then used to determine the cdf of the length of all observed traces in compound windows. In the following, subscripts refer to the simple subwindow of observation and superscripts denote the type of censoring. Thus T_i is the actual length of the trace of a fracture intersecting subwindow i, and T_i^0, T_i^1, and T_i^2 are the actual trace lengths, in subwindow i, that are uncensored, singly or doubly censored, respectively. The corresponding random variables describing the length of traces that intersect the window and are large enough to be recorded will be indicated by the superscript obs.

[15] For uncensored, singly and doubly censored traces, that is, for $j = 0$, 1, and 2, equation (2) is

$$P\left(T_i^{j\,\text{obs}} < t\right) = \iiint_{t_0 \le T_i^j < t} k(\mathbf{s})\mathrm{d}\mathbf{s} \Big/ \iiint_{t_0 \le T_i^j} k(\mathbf{s})\mathrm{d}\mathbf{s} \tag{3}$$

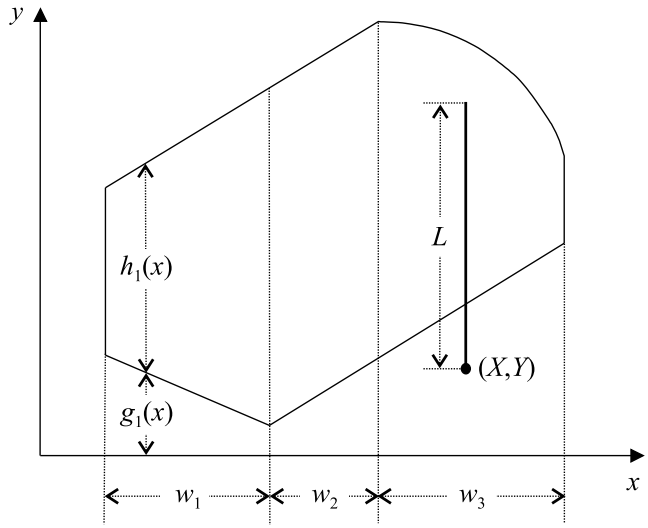

Figure 2. Compound window of observation split into three simple subwindows of widths w_1, w_2, and w_3, respectively. Subwindow 3 is intersected by a fracture of length L and whose lower end has coordinates (X, Y). The height of each subwindow is $h_i(x)$. The distance of the lower edge of each window from the x axis is $g_i(x)$.

The cdf of the length of all traces observed in window i is then given by

$$P\left(T_i^{\text{obs}} < t\right) = \sum_{j=0}^{2} \iiint_{t_0 \le T_i^j < t} k(\mathbf{s})\mathrm{d}\mathbf{s} \Big/ \sum_{j=0}^{2} \iiint_{t_0 \le T_i^j} k(\mathbf{s})\mathrm{d}\mathbf{s} \tag{4}$$

and the cdf of the lengths of all traces in a compound window, comprising n subwindows, is

$$P\left(T^{\text{obs}} < t\right) = \sum_{i=1}^{n} \sum_{j=0}^{2} \iiint_{t_0 \le T_i^j < t} k(\mathbf{s})\mathrm{d}\mathbf{s} \Big/ \sum_{i=1}^{n} \sum_{j=0}^{2} \iiint_{t_0 \le T_i^j} k(\mathbf{s})\mathrm{d}\mathbf{s} \tag{5}$$

4. Observed Trace Length Distribution: Fractures Spatially Characterized by a Uniform Poisson Processes

[16] A common, but not universal, assumption in fracture studies is that of the random spatial distribution of fractures, which is taken here to mean that the distribution of the lower end points of fracture traces can be described by a uniform Poisson process and that the trace length distribution is independent of location. This is equivalent to assuming that X, Y, and L are independent and that X and Y are uniformly distributed. For fracture systems that exhibit significant clustering or anticlustering, the simplification described in this section does not apply. It can be shown (Appendix A) that under the assumption of spatial randomness equation (3) simplifies to

$$P\left(T_i^{j\text{obs}} < t\right) = \iiint_{t_0 \le T_i^j < t} f(l)\mathrm{d}\mathbf{s} \Big/ \iiint_{t_0 \le T_i^j} f(l)\mathrm{d}\mathbf{s} \tag{6}$$

where $f(l)$ is the underlying pdf of fracture trace lengths. Similar simplifications apply to equations (4) and (5). For the purpose of presentation, it is useful to represent the numerator in equation (6) by a function, $G_i^j(t)$, defined so that

$$G_i^j(t) = \iiint_{t_0 \le T_i^j < t} f(l)\mathrm{d}\mathbf{s} \tag{7}$$

The denominator in equation (6) can be decomposed into two parts as follows:

$$\iiint_{t_0 \le T_i^j} f(l)\mathrm{d}\mathbf{s} = \iiint_{T_i^j = h_i^{\max}} f(l)\mathrm{d}\mathbf{s} + \iiint_{t_0 \le T_i^j < h_i^{\max}} f(l)\mathrm{d}\mathbf{s} \tag{8}$$

This is necessary when considering doubly censored traces in windows whose height is constant, that is, when there is a nonzero probability that the observed trace length is $h_i^{\max}$, the (maximum) height of the window. In this case, a constant, I_i^C, is introduced to represent the first term of the right hand side of equation (8). The superscript C denotes merely that I_i^C is a constant. Formally,

$$I_i^C = \begin{cases} \iiint_{T_i^j = h_i^{\max}} f(l)\mathrm{d}\mathbf{s} & j = 2, \quad h_i^{\max} = h_i^{\min} \\ 0 & \text{otherwise} \end{cases} \tag{9}$$

Thus equation (8) can be written as

$$\iiint_{t_0 \le T_i^j} f(l)\mathrm{d}\mathbf{s} = I_i^C + G_i^j\left(h_i^{\max}\right) \tag{10}$$

Combining equations (6), (7), and (10) allows the cdf to be written simply as

$$P\left(T_i^{j\text{obs}} < t\right) = \frac{G_i^j(t)}{I_i^C + G_i^j(h_i^{\max})} \tag{11}$$

It follows that the cdf of the lengths, T_i^{obs}, of all fracture traces observed in subwindow i is given by

$$P\left(T_i^{\text{obs}} < t\right) = \frac{\sum_{j=0}^{2} G_i^j(t)}{I_i^C + \sum_{j=0}^{2} G_i^j(h_i^{\max})} \tag{12}$$

and that the cdf of the lengths, T^{obs}, of the observed traces of all fractures within the full window of observation is given simply by

$$P\left(T^{\text{obs}} < t\right) = \frac{\sum_{i=1}^{n} \sum_{j=0}^{2} G_i^j(t)}{\sum_{i=1}^{n} I_i^C + \sum_{j=0}^{2} G_i^j(h_i^{\max})} \tag{13}$$

If required, the distributions of the lengths of uncensored, singly and doubly censored traces for a compound window can be constructed analogously from equation (11).

[17] In addition, for each window i, the ratios $G_i^0(h_i^{\max}):G_i^1(h_i^{\max}):I_i^C + G_i^2(h_i^{\max})$ are those of the expected numbers of observed traces that are uncensored, singly censored, and doubly censored, respectively.

[18] In order to express the final results compactly, it is useful to express $G_i^j(t)$ in terms of two functions, $I_i^j(\tau)$ and $J_i^j(\tau)$, where the subscript i and the superscript j are defined as in section 3. The theoretical distributions of observed trace lengths can then be constructed from $I_i^j(\tau)$, $J_i^j(\tau)$ and I_i^C, which are derived from the underlying distribution of fracture trace lengths and the geometry of the window of observation. For an observed trace length, t, the dependence of $G_i^j(t)$ on $I_i^j(\tau)$ and $J_i^j(\tau)$ is given explicitly by

$$G_i^j(t) = \begin{cases} 0 & t < t_0 \\ J_i^j(t) - J_i^j(t_0) & t_0 \le t \le h_i^{\min} \\ I_i^j(t) - I_i^j\left(h_i^{\min}\right) + J_i^j\left(h_i^{\min}\right) - J_i^j(t_0) & h_i^{\min} < t \le h_i^{\max} \end{cases} \tag{14}$$

Details of the mathematical development of $I_i^j(\tau)$, $J_i^j(\tau)$ and I_i^C and of their relationship to $G_i^j(t)$ are given in Appendix A.

5. Observed Trace Length Distribution: Simple Windows With Uniformly Varying Heights

5.1. Introduction

[19] Although windows of observation in the field often have complicated outlines, in many cases at least a large section of the window can be divided into a set of directionally nonreentrant windows, with edges that can be approximated by straight lines. In this section, the functions $I_i^j(\tau)$, $J_i^j(\tau)$, and I_i^C are presented for a slightly more general set of simple windows, namely, those whose heights vary uniformly across the width of the window between $h_i^{\min}$ and $h_i^{\max}$. Spatial randomness is assumed throughout.

[20] The functions have been derived for the exponential, finite range power law and lognormal distributions of fracture trace length using the methodology described in section 4 and Appendix A. This derivation is largely elementary, but quite lengthy, so just the final results are given in Figures 3, 4, and 5. Definitions of the underlying fracture length distributions and their parameters are set out below.

5.2. Exponential Fracture Length Distribution

[21] The pdf of an exponential distribution with mean, μ, is given by

$$f(l) = \frac{1}{\mu}\exp\left(-\frac{l}{\mu}\right) \tag{15}$$

where l is the fracture length.

5.3. Power Law Fracture Length Distribution

[22] The power law distribution has two commonly used forms distinguished by the range over which they are defined. The first, defined over a semi-infinite range bounded by a lower cutoff length, l_0, is often given as

$$N = Cl^{-D} \tag{16}$$

where l is the fracture length, D is the length exponent, N is the number of fractures per unit area with length greater than or equal to l, and C is a constant. The total number of fractures per unit area, ρ, is given by N when $l = l_0$, and hence

$$\rho = Cl_0^{-D} \tag{17}$$

The probability that a fracture chosen at random has a length greater than or equal to l is therefore given by

$$P(L \geq l) = \frac{N}{\rho} = \left(\frac{l}{l_0}\right)^{-D} \tag{18}$$

Thus the cdf of fracture lengths, $P(l < L)$, is

$$F(l) = \begin{cases} \dfrac{l_0^{-D} - l^{-D}}{l_0^{-D}} & l \geq l_0 \\ 0 & \text{otherwise} \end{cases} \tag{19}$$

$$I_i^0(\tau) = \frac{w_i}{2(h_i^{\max} - h_i^{\min})} \times \left[-\tau^2 - 2(\mu - h_i^{\max})\tau - h_i^{\max 2} + 2\mu h_i^{\max} - 2\mu^2\right]\exp\left(-\frac{\tau}{\mu}\right)$$

$$J_i^0(\tau) = \frac{w_i}{2}(2\tau + 2\mu - h_i^{\max} - h_i^{\min})\exp\left(-\frac{\tau}{\mu}\right)$$

$$I_i^1(\tau) = \frac{2w_i\mu}{h_i^{\max} - h_i^{\min}}(\tau + \mu - h_i^{\max})\exp\left(-\frac{\tau}{\mu}\right)$$

$$J_i^1(\tau) = -2w_i\mu\exp\left(-\frac{\tau}{\mu}\right)$$

$$I_i^2(\tau) = -\frac{w_i\mu^2}{h_i^{\max} - h_i^{\min}}\exp\left(-\frac{\tau}{\mu}\right)$$

$$J_i^2(\tau) = 0$$

$$I_i^C = w_i\mu\exp\left(-\frac{h_i^{\min}}{\mu}\right)$$

Figure 3. $I_i^j(\tau)$, $J_i^j(\tau)$, and I_i^C for the exponential distribution of fracture trace lengths.

and the pdf is

$$f(l) = \begin{cases} Dl_0^D l^{-(D+1)} & l \geq l_0 \\ 0 & \text{otherwise} \end{cases} \tag{20}$$

The second form of the power law distribution is defined over a finite range bounded by the lower cutoff and an upper cutoff, l_m. In this case, the cdf is given by

$$F(l) = \begin{cases} \dfrac{l_0^{-D} - l^{-D}}{l_0^{-D} - l_m^{-D}} & l_0 \leq l \leq l_m \\ 0 & \text{otherwise} \end{cases} \tag{21}$$

and the pdf is given by

$$f(l) = \begin{cases} \dfrac{Dl^{-(D+1)}}{l_0^{-D} - l_m^{-D}} & l_0 \leq l \leq l_m \\ 0 & \text{otherwise} \end{cases} \tag{22}$$

The mean is given by

$$\int_{l_0}^{l_m} lf(l)dl = \begin{cases} \dfrac{D}{D-1}\dfrac{l_0^{1-D} - l_m^{1-D}}{l_0^{-D} - l_m^{-D}} & D \neq 1 \\ \dfrac{1}{l_0^{-1} - l_m^{-1}}\ln\left(\dfrac{l_m}{l_0}\right) & D = 1 \end{cases} \tag{23}$$

It is clear from the cdfs that the semi-infinite range power law is just the limiting case of the finite range form as the upper cutoff tends to infinity. Thus results are given

For $D \neq 1$ and $D \neq 2$:

$$I_i^0(\tau) = \frac{w_i}{(h_i^{\max} - h_i^{\min})} \frac{1}{(l_0^{-D} - l_m^{-D})} \left[-\frac{D}{2(D-2)} \tau^{2-D} + \frac{D}{D-1} h_i^{\max} \tau^{1-D} - \frac{1}{2} h_i^{\max 2} \tau^{-D} \right]$$

$$J_i^0(\tau) = w_i \frac{1}{(l_0^{-D} - l_m^{-D})} \left[\frac{D}{(D-1)} \tau^{1-D} - \frac{(h_i^{\max} + h_i^{\min})}{2} \tau^{-D} \right]$$

$$I_i^1(\tau) = \frac{w_i}{(h_i^{\max} - h_i^{\min})} \frac{1}{(l_0^{-D} - l_m^{-D})} \left[l_m^{-D} (\tau^2 - 2h_i^{\max} \tau) + \frac{2}{D-2} \tau^{2-D} - \frac{2}{D-1} h_i^{\max} \tau^{1-D} \right]$$

$$J_i^1(\tau) = -w_i \frac{1}{(l_0^{-D} - l_m^{-D})} \left[\frac{2}{D-1} \tau^{1-D} + 2 l_m^{-D} \tau \right]$$

$$I_i^2(\tau) = \frac{w_i}{(h_i^{\max} - h_i^{\min})} \frac{1}{(l_0^{-D} - l_m^{-D})} \left[\frac{1}{2} l_m^{-D} \tau^2 - \frac{D}{D-1} l_m^{1-D} \tau - \frac{1}{(D-1)(D-2)} \tau^{2-D} \right]$$

$$J_i^2(\tau) = 0$$

$$I_i^C = w_i \frac{1}{(l_0^{-D} - l_m^{-D})} \left[\frac{1}{D-1} h_i^{\max 1-D} + h_i^{\max} l_m^{-D} - \frac{D}{D-1} l_m^{1-D} \right]$$

For $D = 2$, the following expressions must be used in place of $I_i^0(\tau)$, $I_i^1(\tau)$, and $I_i^2(\tau)$ in the above:

$$I_i^0(\tau) = \frac{w_i}{(h_i^{\max} - h_i^{\min})} \frac{1}{(l_0^{-2} - l_m^{-2})} \left[\ln \tau + 2h_i^{\max} \tau^{-1} - \frac{1}{2} h_i^{\max 2} \tau^{-2} \right]$$

$$I_i^1(\tau) = \frac{w_i}{(h_i^{\max} - h_i^{\min})} \frac{1}{(l_0^{-2} - l_m^{-2})} \left[l_m^{-2} (\tau^2 - 2h_i^{\max} \tau) - 2\ln(\tau) - 2h_i^{\max} \tau^{-1} \right]$$

$$I_i^2(\tau) = \frac{w_i}{(h_i^{\max} - h_i^{\min})} \frac{1}{(l_0^{-2} - l_m^{-2})} \left[\frac{1}{2} l_m^{-2} \tau^2 - 2 l_m^{-1} \tau + \ln \tau \right]$$

For $D = 1$

$$I_i^0(\tau) = \frac{w_i}{(h_i^{\max} - h_i^{\min})} \frac{1}{(l_0^{-1} - l_m^{-1})} \left[\frac{1}{2} \tau - h_i^{\max} \ln(\tau) - \frac{1}{2} h_i^{\max 2} \tau^{-1} \right]$$

$$J_i^0(\tau) = -w_i \frac{1}{(l_0^{-1} - l_m^{-1})} \left[\ln(\tau) + \frac{(h_i^{\max} + h_i^{\min})}{2} \tau^{-1} \right]$$

$$I_i^1(\tau) = \frac{w_i}{(h_i^{\max} - h_i^{\min})} \frac{1}{(l_0^{-1} - l_m^{-1})} \left[l_m^{-1} \tau^2 - 2(1 + l_m^{-1} h_i^{\max}) \tau + 2h_i^{\max} \ln(\tau) \right]$$

$$J_i^1(\tau) = -2w_i \frac{1}{(l_0^{-1} - l_m^{-1})} \left[l_m^{-1} \tau - \ln(\tau) \right]$$

$$I_i^2(\tau) = \frac{w_i}{2(h_i^{\max} - h_i^{\min})} \frac{1}{(l_0^{-1} - l_m^{-1})} \left[l_m^{-1} \tau^2 + 2 \ln\left(\frac{l_m}{\tau}\right) \tau \right]$$

$$J_i^2(\tau) = 0$$

$$I_i^C = w_i \frac{1}{(l_0^{-1} - l_m^{-1})} \left[l_m^{-1} h_i^{\max} + 1 - \ln\left(\frac{l_m}{h_i^{\max}}\right) \right]$$

Figure 4. $I_i^j(\tau)$, $J_i^j(\tau)$, and I_i^C for the finite range power law distribution of fracture trace lengths.

only for the finite range form (Figure 4): results for the semi-infinite form can be derived simply by considering the limit as l_m tends to infinity. In order to apply the power law distributions to all the fractures under consideration it must be assumed that $t_0 \geq l_0$.

5.4. Lognormal Fracture Length Distribution

[23] The pdf of the lognormal distribution of fracture lengths is

$$f(l) = \frac{1}{\sqrt{2\pi}\sigma l} \exp\left[-\frac{1}{2} \left(\frac{\ln l - \mu}{\sigma} \right)^2 \right] \quad (24)$$

where l is the fracture length, μ is the mean of $\ln l$, and σ is the standard deviation of $\ln l$.

6. Observed Trace Length Distribution: Rectangular Windows

[24] In this section, the formulae from section 5 are applied to an example compound window, namely, a rectangle with sides of length W and H, and with fractures orientated at an acute angle θ to the base of the window (Figure 6). Without loss of generality it can be assumed that $W < H \cos \theta$. The full window is composed of three

$$I_i^0(\tau) = \frac{w_i}{4(h_i^{\max} - h_i^{\min})}\left[h_i^{\max 2}\,\mathrm{erf}\left(\frac{\ln\tau - \mu}{\sigma\sqrt{2}}\right) - 2h_i^{\max}\exp\left(\mu + \frac{1}{2}\sigma^2\right)\mathrm{erf}\left(\frac{\ln\tau - \mu - \sigma^2}{\sigma\sqrt{2}}\right) + \exp(2\mu + 2\sigma^2)\,\mathrm{erf}\left(\frac{\ln\tau - \mu - 2\sigma^2}{\sigma\sqrt{2}}\right)\right]$$

$$J_i^0(\tau) = \frac{w_i}{2}\left[\frac{h_i^{\max} + h_i^{\min}}{2}\,\mathrm{erf}\left(\frac{\ln\tau - \mu}{\sigma\sqrt{2}}\right) - \exp\left(\mu + \frac{1}{2}\sigma^2\right)\mathrm{erf}\left(\frac{\ln\tau - \mu - \sigma^2}{\sigma\sqrt{2}}\right)\right]$$

$$I_i^1(\tau) = \frac{w_i}{2(h_i^{\max} - h_i^{\min})}\left[-\tau(\tau - 2h_i^{\max})\,\mathrm{erfc}\left(\frac{\ln\tau - \mu}{\sigma\sqrt{2}}\right) + 2h_i^{\max}\exp\left(\mu + \frac{1}{2}\sigma^2\right)\mathrm{erf}\left(\frac{\ln\tau - \mu - \sigma^2}{\sigma\sqrt{2}}\right) - \exp(2\mu + 2\sigma^2)\,\mathrm{erf}\left(\frac{\ln\tau - \mu - 2\sigma^2}{\sigma\sqrt{2}}\right)\right]$$

$$J_i^1(\tau) = w_i\left[\tau\,\mathrm{erfc}\left(\frac{\ln\tau - \mu}{\sigma\sqrt{2}}\right) + \exp\left(\mu + \frac{1}{2}\sigma^2\right)\mathrm{erf}\left(\frac{\ln\tau - \mu - \sigma^2}{\sigma\sqrt{2}}\right)\right]$$

$$I_i^2(\tau) = \frac{w_i}{4(h_i^{\max} - h_i^{\min})}\left[-\tau^2\,\mathrm{erfc}\left(\frac{\ln\tau - \mu}{\sigma\sqrt{2}}\right) + 2\tau\exp\left(\mu + \frac{1}{2}\sigma^2\right)\mathrm{erfc}\left(\frac{\ln\tau - \mu - \sigma^2}{\sigma\sqrt{2}}\right) + \exp(2\mu + 2\sigma^2)\,\mathrm{erf}\left(\frac{\ln\tau - \mu - 2\sigma^2}{\sigma\sqrt{2}}\right)\right]$$

$$J_i^2(\tau) = 0$$

$$I_i^C = \frac{w_i}{2}\left[-h_i^{\min}\,\mathrm{erfc}\left(\frac{\ln h_i^{\min} - \mu}{\sigma\sqrt{2}}\right) + \exp\left(\mu + \frac{1}{2}\sigma^2\right)\mathrm{erfc}\left(\frac{\ln h_i^{\min} - \mu - \sigma^2}{\sigma\sqrt{2}}\right)\right]$$

Figure 5. $I_i^j(\tau)$, $J_i^j(\tau)$, and I_i^C for the lognormal distribution of fracture trace lengths.

directionally nonreentrant subwindows and two areas too small to contain a recordable fracture trace. Calculation of the observed trace length distributions is simply a matter of substitution of the appropriate values of $h_i^{\min}$, $h_i^{\max}$, and w_i into the formulae in Figure 3, 4, or 5, to give $I_i^j(\tau)$, $J_i^j(\tau)$, and I_i^C; using $I_i^j(\tau)$, $J_i^j(\tau)$ to evaluate $G_i^j(t)$ from equation (14); and finally using I_i^C and $G_i^j(t)$ in equation (13) to produce the cdf. The minimum and maximum heights for each subwindow are

$$\begin{aligned} h_1^{\min} &= t_0 & h_1^{\max} &= \frac{H}{\sin\theta} \\ h_2^{\min} &= \frac{H}{\sin\theta} & h_2^{\max} &= \frac{H}{\sin\theta} \\ h_3^{\min} &= t_0 & h_3^{\max} &= \frac{H}{\sin\theta} \end{aligned} \tag{25}$$

and the widths are

$$\begin{aligned} w_1 &= H\cos\theta - t_0\sin\theta\cos\theta \\ w_2 &= W\sin\theta - H\cos\theta \\ w_3 &= H\cos\theta - t_0\sin\theta\cos\theta \end{aligned} \tag{26}$$

Since the height of window 2 is constant, I_2^C is nonzero. From equation (13), the cdf of the trace lengths of all fractures intersecting the entire window can be expressed simply as

$$P(T^{\mathrm{obs}} < t) = \frac{\sum_{i=1}^{3}\sum_{j=0}^{2} G_i^j(t)}{I_2^C + \sum_{i=1}^{3}\sum_{j=0}^{2} G_i^j\left(\frac{H}{\sin\theta}\right)} \tag{27}$$

It is clear that windows 1 and 3 have identical characteristics and hence $G_1^j(t)$ and $G_3^j(t)$ are equal. In addition, the minimum height of windows 1 and 3 is defined by the lower truncation limit and so, from equation (14), $G_i^j(t)$ is equal to $I_i^j(t) - I_i^j(t_0)$, for $i = 1$ or 3. The resulting cdf is conveniently presented as

$$P(T^{\mathrm{obs}} < t) = \frac{R(t) - R(t_0)}{S - R(t_0)} \tag{28}$$

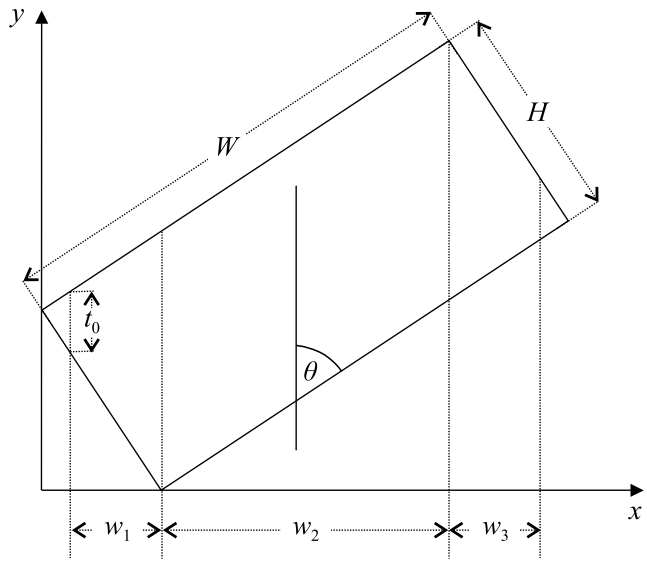

Figure 6. Rectangular window of observation split into three simple subwindows of widths w_1, w_2, and w_3.

where the function $R(\tau)$ and the constant S are given in Figure 7 for the three underlying distributions considered.

[25] The functions in Figure 7 describe the cdf of trace lengths observed in a rectangular window completely, and for arbitrary windows equivalent functions can be derived in a similar manner. However, if only numerical values of a cdf are required, it is generally quicker to avoid such algebraic manipulations and calculate the cdf directly from evaluations of $I_i^j(\tau)$, $J_i^j(\tau)$, and I_i^C, which can be achieved simply in a spreadsheet.

7. Distribution of the Number of Observed Fracture Traces

7.1. Fractures With Spatial Density Described by a Uniform Poisson Process

[26] The causes of bias in the estimation of the parameters of trace length distributions, i.e., the finite window and systematic truncation, also affect estimation of the underlying fracture density, ρ. In this section, the distribution of the number of traces observed in the window is presented for the three underlying distributions of fracture trace length considered in section 5.

[27] Consider a region with area A, bounded by $0 < x < w_i$, in which fractures are uniformly distributed. The mean number of fractures, n_i, with lower ends in the region is

$$n_i = \rho A \tag{29}$$

and the probability, p_i, that a fracture (with its lower end in the region) chosen at random is observed in the window, i, is constant and given by

$$p_i = P(t_0 \le T_i) = \frac{1}{A}\iiint_{t_0 \le T_i} f(l)\mathrm{d}\mathbf{s} = \frac{1}{A}\left[I_i^C + \sum_{j=0}^{2} G_i^j\left(h_i^{\max}\right)\right] \tag{30}$$

Hence the number of traces observed in the window is binomially distributed with mean:

$$\mu_i^{\mathrm{obs}} = n_i p_i = \rho\left[I_i^C + \sum_{j=0}^{2} G_i^j\left(h_i^{\max}\right)\right] \tag{31}$$

and variance

$$\begin{aligned}\left(\sigma_i^{\mathrm{obs}}\right)^2 &= \lim_{A\to\infty} n_i p_i(1-p_i)\\ &= n_i p_i\\ &= \mu_i^{\mathrm{obs}}\end{aligned} \tag{32}$$

It follows that for a compound window, the number of observed traces has a binomial distribution with mean and variance

$$\mu^{\mathrm{obs}} = \left(\sigma^{\mathrm{obs}}\right)^2 = \rho\left[\sum_{i=1}^{n} I_i^C + \sum_{j=0}^{2} G_i^j\left(h_i^{\max}\right)\right] \tag{33}$$

Consequently, if the number of fracture traces is large, the number of observed traces can be considered to have a Normal distribution with mean and variance μ^{obs}.

7.2. Simple Windows With Uniformly Varying Heights

[28] The mean of the distribution of the number of traces observed in a window with uniformly varying height is given in Figure 8 for the exponential, finite range power law and lognormal distributions.

8. Discussion

8.1. Comments on the Semi-infinite Range Power Law Distribution

[29] The quantification of the distributions of observed trace lengths and the number of observed traces allows several observations to be made about the application of power law models of fracture length, and in particular, the much used semi-infinite range form. Formulae for the semi-infinite range power law can be derived simply from Figure 4 by letting the upper cutoff, l_m, tend to infinity. Since l_m always appears to a negative power, this can be achieved simply by setting all terms containing a factor of l_m to zero. Similar discussion of the exponential, lognormal and finite range power law is facilitated by the results in Figures 3, 4, 5, 7, and 8 but is not included here.

8.1.1. Trace Lengths

[30] First, it is interesting to note that when the exponent in the semi-infinite range power law is equal to 2, and the window of observation has a constant height, there is no censoring bias at all, provided all traces are included in the analysis. For windows of constant height, the strategy of ignoring censored traces introduces bias. This decreases as D takes larger values but, for values of D typically reported in the literature, the bias generally remains larger than that produced by the alternative approach of including all traces. For example, Figure 9 compares the mean error when the underlying cdf of trace lengths is estimated first by the cdf of all observed traces and then by the cdf of uncensored trace lengths only. The error is taken to be the value of the estimated cdf minus the value of the underlying cdf. The window has a constant height ten times the lower truncation limit, which is taken to be one.

[31] If all traces are included in the analysis, the bias in a window of constant height increases as D differs from 2. Figure 10 shows the cdfs of observed trace lengths (solid lines) on a typical log-log plot of power law results for values of D equal to 1.2, 1.4, 2.0, 2.4, and 2.8 in a window whose height is ten times the unit lower truncation limit. If the lower cutoff is taken to be equal to the lower truncation limit, these values of D give mean fracture trace lengths of 6.00, 3.50, 2.00, 1.71, and 1.56 length units, respectively. The dashed lines show the representations of the underlying power law for each value of D. The curvature of the solid lines increases as D differs from 2, but the deviation from the unbiased curves is greater for values of D less than 2. This is simply because the mean trace length varies increasingly rapidly with D as it approaches 1, and hence the expected proportion of the number of traces that are censored also increases more quickly. For values of D as large as 2.8 the deviation is not great even though the standardized cumulative frequency ranges over 3 orders of magnitude, whereas for small values of D, large errors are seen even with a small range in cumulative frequency. For values of D close to 2, which are often reported, and particularly for those slightly greater than 2 the deviation from straight-line behavior is small and gradual. For all values of D, it is clear that the deviation from straight-line

Exponential fracture length distribution

$$R(\tau) = \left[-\sin\theta\cos\theta\tau^2 + (W\sin\theta + H\cos\theta - 2\mu\sin\theta\cos\theta)\tau - \mu(W\sin\theta + H\cos\theta) - HW\right]\exp\left(-\frac{\tau}{\mu}\right)$$

$$S = 0$$

Finite range power law fracture length distribution

For $D \neq 1$ and $D \neq 2$

$$R(\tau) = 3l_m^{-D}\sin\theta\cos\theta\tau^2 + 2l_m^{-D}(W\sin\theta - 3H\cos\theta)\tau - \frac{2D}{D-1}l_m^{1-D}\sin\theta\cos\theta\tau - \frac{D-3}{D-1}\sin\theta\cos\theta\tau^{2-D} + \frac{D-2}{D-1}(W\sin\theta + H\cos\theta)\tau^{1-D} - HW\tau^{-D}$$

$$S = \frac{H}{\sin\theta}(3W\sin\theta - 4H\cos\theta)l_m^{-D} - \frac{D}{D-1}(W\sin\theta + H\cos\theta)l_m^{1-D}$$

For $D = 1$

$$R(\tau) = 3l_m^{-1}\sin\theta\cos\theta\tau^2 - 2l_m^{-1}(W\sin\theta + H\cos\theta)\tau - \left[3 - 2\ln\left(\frac{l_m}{\tau}\right)\right]\sin\theta\cos\theta\tau + (W\sin\theta + H\cos\theta)\ln(\tau) - HW\tau^{-1}$$

$$S = 2H\left[\ln(l_m) - 2\right]\cos\theta + (W\sin\theta - H\cos\theta)\ln\left(\frac{H^2}{l_m\sin^2\theta}\right) - l_m^{-1}HW$$

For $D = 2$

$$R(\tau) = 3l_m^{-2}\sin\theta\cos\theta\tau^2 + 2l_m^{-2}(W\sin\theta - 3H\cos\theta)\tau - 4l_m^{-1}\sin\theta\cos\theta\tau + 8\sin\theta\cos\theta\ln\tau - HW\tau^{-2}$$

$$S = \frac{H}{\sin\theta}(3W\sin\theta - 4H\cos\theta)l_m^{-2} - 2(W\sin\theta + H\cos\theta)l_m^{-1} + \sin\theta\cos\theta\left[1 - 8\ln\left(\frac{H}{\sin\theta}\right)\right]$$

Lognormal fracture length distribution

$$R(\tau) = \left[\frac{3}{2}\sin\theta\cos\theta\tau^2 - (W\sin\theta + H\cos\theta)\tau + HW\right]\mathrm{erf}\left(\frac{\ln\tau - \mu}{\sigma\sqrt{2}}\right) - \frac{1}{2}\left[2\sin\theta\cos\theta\tau - (W\sin\theta + H\cos\theta)\right]\exp\left(\mu + \frac{1}{2}\sigma^2\right)\mathrm{erf}\left(\frac{\ln\tau - \mu - \sigma^2}{\sigma\sqrt{2}}\right) - \frac{3}{2}\sin\theta\cos\theta\tau^2 + \left[\exp\left(\mu + \frac{1}{2}\sigma^2\right)\sin\theta\cos\theta + W\sin\theta + H\cos\theta\right]\tau$$

$$S = \frac{1}{2}(W\sin + H\cos)\exp\left(\mu + \frac{1}{2}\sigma^2\right) + \frac{HW}{2}$$

Figure 7. $R(\tau)$ and S for a rectangular window of observation.

behavior starts from $L = t_0 = 1$ and that there is not, as is sometimes assumed, a straight-line segment followed by an abrupt change in slope. Comparison of the observed and underlying cdfs for D equal to 1.2 and 2.8 highlights the size and nature of the bias for values greater than or less than 2 (Figure 11). Note that the solid and dashed lines representing the cdfs for D = 2.8 are almost indistinguishable.

[32] Greater bias is introduced as the minimum window heights decreases. Figure 12 shows log-log plots for the same parameter values as those shown in Figure 10 but for the extreme case of a window whose height varies uniformly between 1 and 10. As in the case of a window of constant height, deviation from straight-line behavior starts at $L = t_0 = 1$ and increases with L. Nowhere is the graph straight. Incorrectly identifying a straight portion of the

Exponential fracture length distribution

$$\mu_i^{\text{obs}} = \rho w_i \left[\frac{h_i^{\max} + h_i^{\min}}{2} + \mu - t_0 \right] \exp\left(-\frac{t_0}{\mu} \right)$$

Finite range power law fracture length distribution

$$\mu_i^{\text{obs}} = \rho w_i \frac{1}{(l_0^{-D} - l_m^{-D})} \left[\left(\frac{h_i^{\max} + h_i^{\min}}{2} \right) (t_0^{-D} - l_m^{-D}) - \frac{(D-2)}{(D-1)} t_0^{1-D} + 2 t_0 l_m^{-D} - \frac{D}{(D-1)} l_m^{1-D} \right]$$

Lognormal fracture length distribution

$$\mu_i^{\text{obs}} = \frac{\rho w_i}{2} \left[\left(\frac{h_i^{\max} + h_i^{\min}}{2} - 2t_0 \right) \operatorname{erfc}\left(\frac{\ln t_0 - \mu}{\sigma\sqrt{2}} \right) + \exp\left(\mu + \frac{1}{2}\sigma^2 \right) \operatorname{erfc}\left(\frac{\ln t_0 - \mu - \sigma^2}{\sigma\sqrt{2}} \right) \right]$$

Figure 8. Mean number of fractures observed in a simple window with uniformly varying height.

curve and fitting a straight line will tend to produce underestimates of D for values of D less than 2 and overestimates if D is greater than 2. The observed and underlying cdfs for D equal to 1.2 and 2.8 are shown in Figure 13, illustrating that the underestimation problem is the more acute.

[33] It is perhaps worth emphasizing here the permissible range of values of D in the semi-infinite range power law. Values less than or equal to one have been reported occasionally in the literature and such values are mathematically acceptable in the sense that equation (19) describes a valid cdf for all values of D greater than zero. However, if D is less than or equal to one, its value cannot be correctly inferred from field data acquired in a finite window since, in this case, the cdf of observed trace lengths is (from Figure 4) either

$$P(T_i^{\text{obs}} < t) = \begin{cases} 0 & t < h_i^{\min} \\ \dfrac{t - h_i^{\min}}{h_i^{\max} - h_i^{\min}} & h_i^{\min} \le t < h_i^{\max} \\ 1 & h_i^{\max} \le t \end{cases} \tag{34}$$

when $h_i^{\max} \neq h_i^{\min}$, or

$$P(T_i^{\text{obs}} < t) = \begin{cases} 0 & t < h_i^{\max} \\ 1 & h_i^{\max} \le t \end{cases} \tag{35}$$

otherwise, both of which are independent of D. This is a direct consequence of the nonfinite mean of the underlying distribution for $D \le 1$, which results in any sample of the distribution taken in a finite window containing an overwhelming number of doubly censored fracture traces. This can also be seen directly by considering the ratios $I_i^C + G_i^2(h_i^{\max}):G_i^0(h_i^{\max})$ and $I_i^C + G_i^2(h_i^{\max}):G_i^1(h_i^{\max})$ which increase without limit as D approaches 1 from above. Finite range power law behavior with an exponent less than or equal to one is possible, but requires an upper cutoff to be defined and reported.

8.1.2. Fracture Density

[34] The bias involved in estimating fracture density can be determined from the formulae in Figure 8. Figure 14 shows the ratio of the mean density of observed fracture traces to the actual density of fracture traces plotted against the power law exponent for a range of standardized window heights, $\overline{H}$, which expresses the mean height as a multiple of the lower truncation limit, t_0. The lower truncation limit and the lower cutoff are taken to be equal, in which case the magnitude of the fractional bias is less than or equal to α for values of D in the range

$$\frac{2 + \alpha\overline{H}}{1 + \alpha\overline{H}} \le D \le \frac{2 - \alpha\overline{H}}{1 - \alpha\overline{H}} \tag{36}$$

Thus, for example, for a mean window height of 100 times the lower cutoff, the bias is less than 1% for values of D greater than 1.5. Clearly, for zero bias D must be equal to 2.

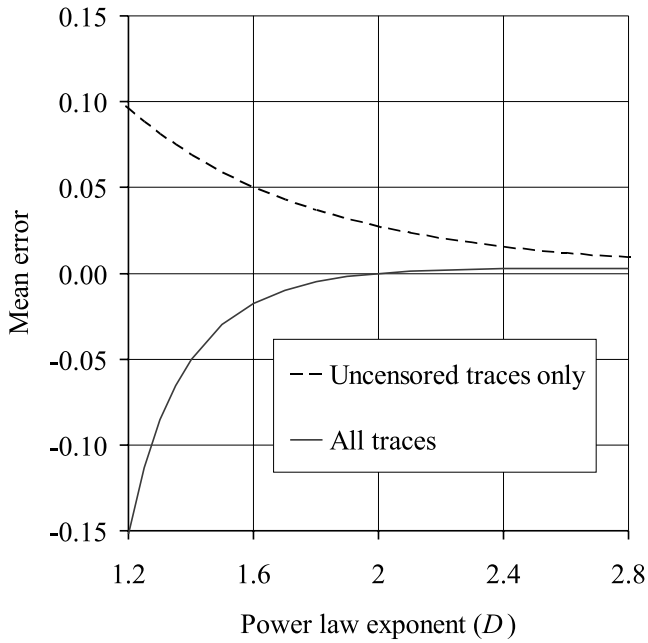

Figure 9. Mean error in estimates of the underlying semi-infinite range power law cdf as a function of exponent D using all traces and uncensored traces only ($h_i^{\max} = h_i^{\min} = 10t_0$.

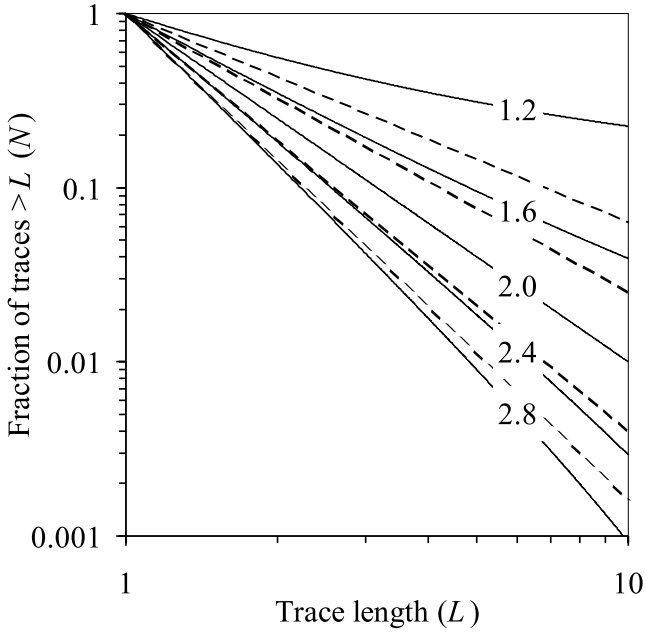

Figure 10. Theoretical distribution of observed trace lengths (solid lines) for D = 1.2, 1.6, 2.0, 2.4, and 2.8. Semi-infinite range power law distribution (dashed lines) for the same values of D; $h_i^{\max} = h_i^{\min} = 10t_0$.

[35] The observed trace length distribution is independent of the lower cutoff, l_0, provided that $l_0 \leq t_0$, but the ratio t_0/l_0 has a significant influence on the estimation of fracture density. The ratio of the mean density of observed fracture traces to the actual density of fracture traces is given by

$$\frac{\text{mean observed density}}{\text{actual density}} = \left(\frac{t_0}{l_0}\right)^{-D}\left[1 - \left(\frac{D-2}{D-1}\right)\frac{1}{\overline{H}}\right] \qquad (37)$$

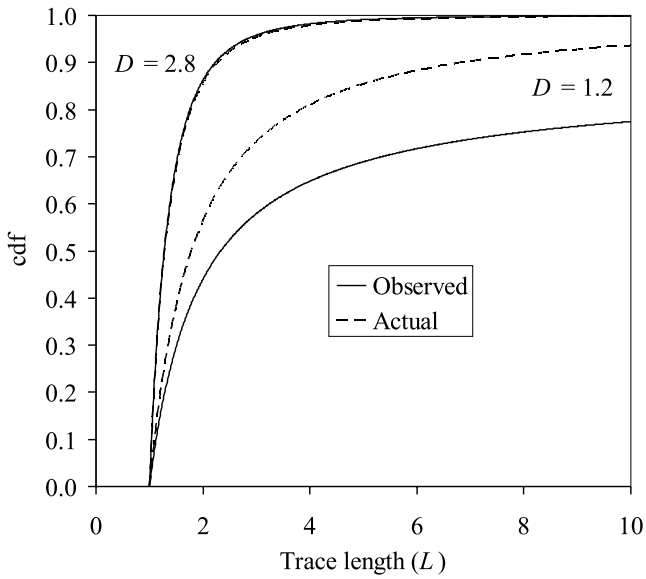

Figure 11. Observed and actual trace length cdfs for the semi-infinite range power law distribution for D = 1.2 and 2.8;. $h_i^{\max} = h_i^{\min} = 10t_0$.

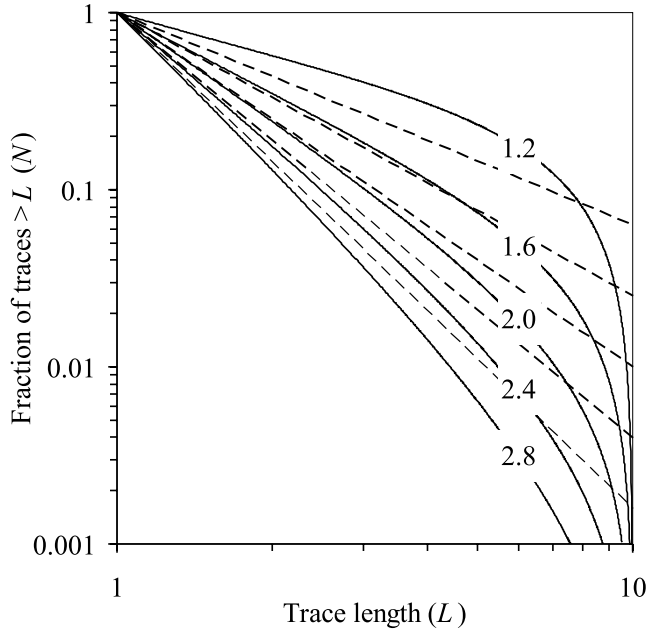

Figure 12. Theoretical distribution of observed trace lengths (solid lines) for D = 1.2, 1.6, 2.0, 2.4, and 2.8. Semi-infinite range power law distribution (dashed lines) for the same values of D; $h_i^{\max} = 10t_0$ and $h_i^{\min} = t_0$.

Figure 15 shows the expression in equation (37) plotted against the power law exponent for a range of values of t_0/l_0. $\overline{H}$ is taken to be 512. As expected, the bias increases as t_0/l_0 increases from one. In the analysis of a single fracture map, bias can be reduced to a minimum by assuming that l_0 is the same as t_0 and then inferring ρ_{l_0}, the density of fractures longer than l_0. However, when a number of maps are to be analyzed, fracture density estimates from maps based upon larger values of t_0 must be corrected to the assumed value of l_0, determined from the smallest value of

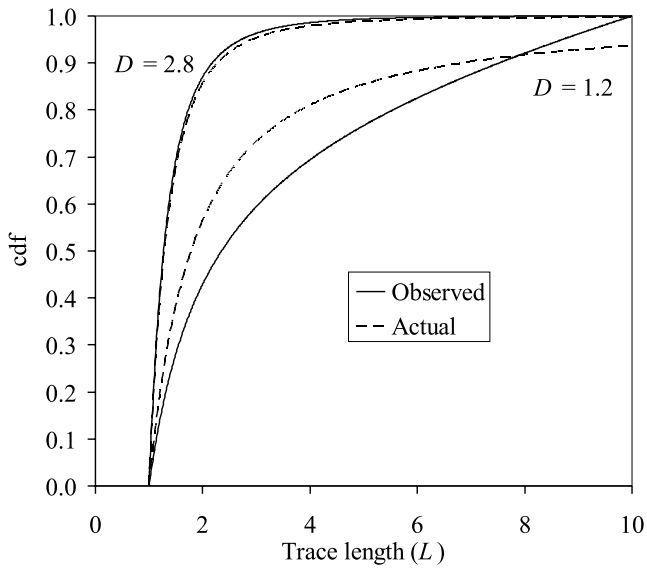

Figure 13. Observed and actual trace length cdfs for the semi-infinite range power law distribution for D = 1.2 and 2.8; $h_i^{\max} = 10t_0$ and $h_i^{\min} = t_0$.

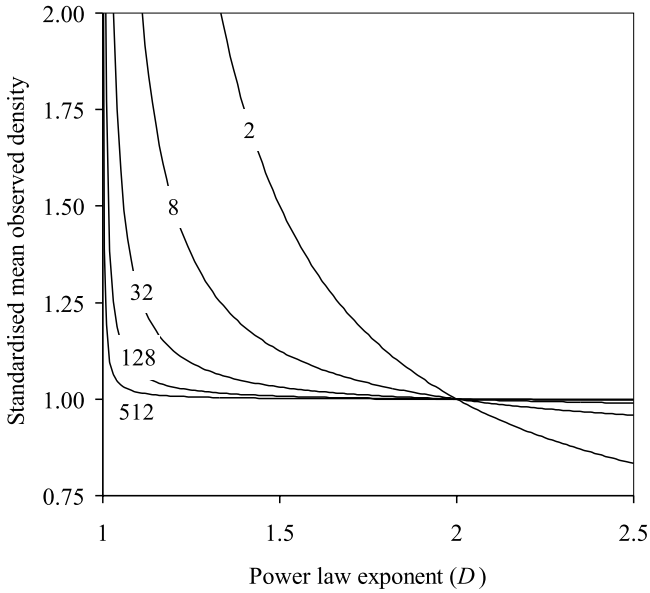

Figure 14. Ratio of mean observed to actual trace density as a function of semi-infinite range power law exponent for $t_0 = l_0$ and $(h_i^{max} + h_i^{min})/2t_0 = 2$, 8, 32, 128, and 512.

t_0. This can be achieved by applying equation (37) provided an estimate of D has been determined.

8.2. Combining Field Results Collected at Different Scales

[36] It is sometimes the case that field mapping investigations are undertaken at substantially different spatial scales. Small-scale site investigations may be supplemented, for example, by the results of an aerial photographic survey. Analysis of the results of such combined investigations must be carried out with some care. Not only are the windows of observation different sizes and almost certainly different shapes, but also the lower truncation limit, t_0, depends upon the resolution of the method of data acquisition. The results in this paper clearly apply to each site individually, but it is also true that they can be applied to the combined results by considering the sites as a compound window, provided the window so formed is directionally nonreentrant. Although the cdfs derived in this paper have been expressed in terms of a common lower truncation limit, the results are equally valid if different limits are taken in each subwindow and hence between sites with different data acquisition strategies and technologies. Even so, there are outstanding issues relating to the analysis of such data. It is the case, for example, that different trace lengths may be recorded for the same fracture when it is observed at different scales. Where this effect is marked, it is necessary to invoke a model describing the relationship between resolution, observed trace length and underlying trace length [e.g., *Odling*, 1997] to account for it.

9. Summary and Conclusions

[37] This paper describes a general methodology for determining the theoretical distributions of observed fracture trace length and number for a large class of finite windows of observation, based upon underlying fracture length distributions, and taking into account edge effects and the lower truncation limit of observation. In particular, detailed results have been presented for areas in which the spatial distribution of fractures can be described by a uniform Poisson process and in which the window of observation can be represented by a collection of subwindows with uniformly varying heights. The cdfs of uncensored, singly censored and doubly censored fracture traces can also be derived from the formulae presented.

[38] The construction of the distributions of observed trace lengths can be achieved by (1) dividing the window of observation into suitable subwindows, $i = 1, \ldots n$, with heights that vary approximately uniformly, (2) substituting, h_i^{max}, h_i^{min} and w_i for each subwindow, i, into the equations in Figure 3, 4, or 5 to give I_i^C, and $I_i^j(\tau)$ and $J_i^j(\tau)$ for $j = 0$, 1 and 2, (3) substituting $I_i^j(\tau)$ and $J_i^j(\tau)$, into equation (14) to give $G_i^j(t)$, and (4) substituting I_i^C and $G_i^j(t)$ into equation (13). However, unless an explicit formula is required for the distribution, it is quicker to avoid the algebraic manipulation in steps 1 to 4, and to perform the above sequence numerically. An example EXCEL spreadsheet performing these calculations is freely available from the author. The number of observed traces for windows with uniformly varying heights is binomially distributed with means and variances given in Figure 8.

[39] Both the size and shape of the window of observation influence the distribution of observed trace lengths and should therefore be reported in detail with the underlying distribution and its inferred parameter values. Similarly, the use of the finite range power law requires both upper and lower cutoffs to be reported.

[40] Analyzing fracture data assuming a semi-infinite range power law length distribution and employing the typical log-log plot approach produces estimates of D that are increasingly inaccurate as the true value of D decreases from 2. An alternative approach is first to estimate D using, for example, the method of *Laslett* [1982b] or by using

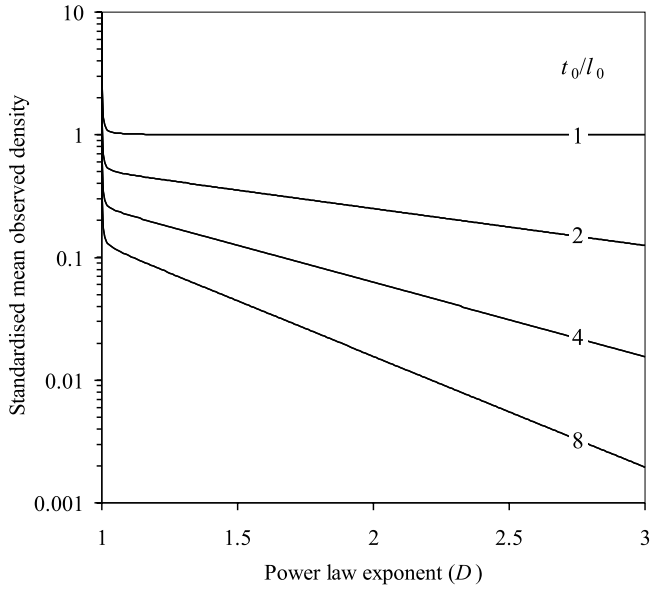

Figure 15. Ratio of mean observed to actual trace density as a function of semi-infinite range power law exponent for $(h_i^{max} + h_i^{min})/2t_0 = 512$, and $t_0/l_0 = 1$, 2, 4, and 8.

simple optimization techniques to fit the theoretical cdf outlined in Figure 4 and then to estimate fracture density using the result in Figure 8.

[41] Although the formulae presented in this paper allow the construction of distributions of fracture trace length and number, there are many issues left to resolve. Clustering, anticlustering, the distribution of fracture orientations within a set, and correlations between length and orientation are all issues that might be addressed statistically. There are also significant uncertainties relating to field investigations that need to be addressed if reliable estimates of the underlying length distribution and its parameters are to be obtained. The inconsistent identification of a break in the rock as a single fracture or set of interconnecting fractures by different investigators and investigation techniques applicable at different scales remains a major source of uncertainty.

Appendix A: Observed Trace Length Distribution: Fractures Generated by a Uniform Poisson Processes

A1. Introduction

[42] In this appendix, the integrals in equation (6) are expressed as repeated integrals with appropriate limits (sections A2 to A4), which can then be evaluated for each underlying trace length distribution. The limits of integration are determined by the conditions under which a fracture trace is either uncensored, or singly or doubly censored, and these are laid out in this section. The functions $I_i^j(\tau)$, $J_i^j(\tau)$, which are required for presentation of the results, are formally defined.

A1.1. Characterization of Censoring

[43] As defined in section 3, the random variables, T_i^0, T_i^1, and T_i^2 represent the actual trace lengths, in subwindow i, that are uncensored, singly or doubly censored, respectively. In addition, the set of lengths of singly censored traces can be partitioned into those lengths censored by just the upper edge of the window, T_i^{1U}, and those censored by just the lower edge, T_i^{1L}. The actual trace lengths in subwindow i are then given by

$$T_i^0 = l \qquad y + l < g_i(x) + h_i(x) \quad y > g_i(x) \tag{A1a}$$

$$T_i^{1U} = h_i(x) - y \qquad y + l > g_i(x) + h_i(x) \quad y \geq g_i(x) \tag{A1b}$$

$$T_i^{1L} = y + l \qquad y + l < g_i(x) + h_i(x) \quad y \leq g_i(x) \tag{A1c}$$

$$T_i^2 = h_i(x) \qquad y + l \geq g_i(x) + h_i(x) \quad y \leq g_i(x) \tag{A1d}$$

$$T_i^j = 0 \qquad \forall\, j \qquad \text{otherwise} \tag{A1e}$$

A1.2. Spatial Randomness and Local Coordinate System

[44] In the following, it is assumed that fractures are spatially distributed according to a uniform Poisson process and that the fracture trace length, L is independent of X and Y and has pdf, $f(l)$. For a single subwindow, i, the spatial randomness assumption allows the replacement of the global coordinate system, $\mathbf{s} = (x, y, l)$, by a coordinate system, $\boldsymbol{\sigma} = (\xi, \psi, \lambda)$, local to the subwindow (Figure A1). Since the height of each subwindow is either constant or varies monotonically between minimum and maximum heights, $h_i^{\min}$ and $h_i^{\max}$, respectively, it is possible to standardize and simplify presentation by defining the origin of the local system to be coincident with the widest end of the window, and by defining the axes such that points in the window have positive coordinates. Furthermore, without loss of generality, the local coordinate system can be constructed so that the surface $y = g_i(x)$ maps to $\psi = 0$. The local coordinate system is then defined by the transformations:

$$\begin{aligned} \xi &= \begin{cases} b_i - x & h_i \text{ increasing} \\ x - a_i & h_i \text{ nonincreasing} \end{cases} \\ \psi &= y - g_i(x) \\ \lambda &= l \end{aligned} \tag{A2}$$

[45] For a region with area A, bounded by $0 \leq \xi \leq w_i$ and containing the lower end of fractures, the assumption of spatial randomness implies that the joint pdf of X, Y, and L is given by

$$k(\boldsymbol{\sigma}) = f(\lambda)/A \tag{A3}$$

and so equation (6) can be rewritten as

$$P\left(T_i^{\text{obs}} < t\right) = \iiint\limits_{t_0 \leq T_i^j < t} f(\lambda)\mathrm{d}\boldsymbol{\sigma} \Bigg/ \iiint\limits_{t_0 \leq T_i^j} f(\lambda)\mathrm{d}\boldsymbol{\sigma} \tag{A4}$$

A1.3. Definition of $I_i^j(\tau)$ and $J_i^j(\tau)$

[46] It will be seen in section A2 that evaluation of the integrals in equation (A4) differs fundamentally depending upon whether t is greater or less than $h_i^{\min}$, and so, for practical purposes, the integrals have to be expressed in terms of the sum of their values over the two ranges of t. Thus

$$\iiint\limits_{t_0 \leq T_i^j < t} f(\lambda)\mathrm{d}\boldsymbol{\sigma} = \begin{cases} \displaystyle\iiint\limits_{h_i^{\min} \leq T_i^j < t} f(\lambda)\mathrm{d}\boldsymbol{\sigma} + \iiint\limits_{t_0 \leq T_i^j < h_i^{\min}} f(\lambda)\mathrm{d}\boldsymbol{\sigma} & h_i^{\min} < t \leq h_i^{\max} \\ \displaystyle\iiint\limits_{t_0 \leq T_i^j < t} f(\lambda)\mathrm{d}\boldsymbol{\sigma} & t_0 \leq t \leq h_i^{\min} \\ 0 & \text{otherwise} \end{cases} \tag{A5}$$

The functions $I_i^j(\tau)$ and $J_i^j(\tau)$ are introduced such that

$$I_i^j(t) - I_i^j\left(h_i^{\min}\right) = \begin{cases} \displaystyle\iiint\limits_{h_i^{\min} \leq T_i^j < t} f(\lambda)\mathrm{d}\boldsymbol{\sigma} & h_i^{\min} < t \leq h_i^{\max} \\ 0 & \text{otherwise} \end{cases} \tag{A6}$$

$$J_i^j(t) - J_i^j(t_0) = \begin{cases} \displaystyle\iiint\limits_{t_0 \leq T_i^j < t} f(\lambda)\mathrm{d}\sigma & t_0 \leq t \leq h_i^{\min} \\ 0 & \text{otherwise} \end{cases} \tag{A7}$$

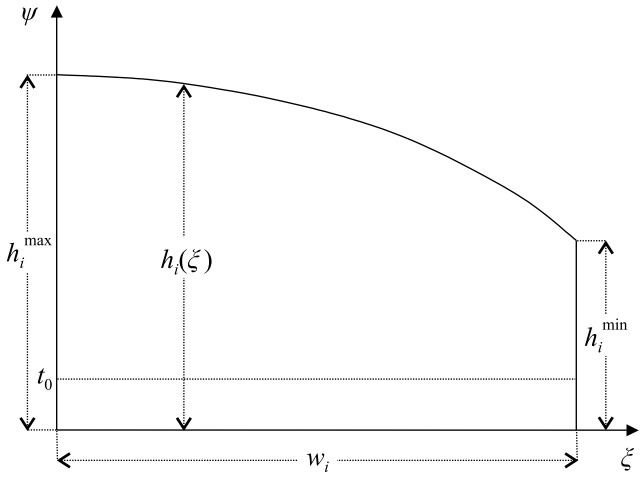

Figure A1. Simple window referenced by local coordinates.

equations (A6) and (A7) do not define $I_i^j(\tau)$ and $J_i^j(\tau)$ uniquely. To complete the definition, it is necessary to specify the value of any constant terms appearing in them. These are taken here to be zero.

A2. Trace Length Distribution of Uncensored Fractures

[47] In terms of local coordinates, a fracture intersects the window and is uncensored when the following inequalities are satisfied:

$$\begin{gathered}\psi + \lambda < h_i(\xi) \\ 0 < \psi \\ 0 \le \xi \le w_i\end{gathered} \tag{A8}$$

in which case the trace length is λ (equation (A1a)). The integral of $f(\lambda)$ over the region defined by the above inequalities and $t_0 \le \lambda < t$ is shown shaded in Figure A2. It can be seen that the region over which the integrals are evaluated comprises two subregions, separated by the plane $\lambda = h_i^{min}$. If h_i is strictly monotonic, the range of ξ above $\lambda = h_i^{min}$ is given by

$$0 \le \xi < h_i^{-1}(\lambda) \tag{A9}$$

where $h_i^{-1}(\lambda)$ in the inverse of $h_i(\xi)$. Alternatively, if h_i is constant or $\lambda < h_i^{min}$, the limits on ξ are determined by the width of the window in the ξ direction. The integral over the region above the plane $\lambda = h_i^{min}$ (which is degenerate if h_i is constant) is

$$I_i^0(t) - I_i^0\left(h_i^{min}\right) = \begin{cases} \int_{h_i^{min}}^{t} \int_0^{h_i^{-1}(\lambda)} \int_0^{h_i(\xi)-\lambda} f(\lambda) d\psi d\xi d\lambda & h_i^{min} < t \le h_i^{max} \\ 0 & \text{otherwise} \end{cases} \tag{A10}$$

The integral over the region below the plane is

$$J_i^0(t) - J_i^0(t_0) = \begin{cases} \int_0^{t} \int_0^{w_i} \int_0^{h_i(\xi)-\lambda} f(\lambda) d\psi d\xi d\lambda & t_0 \le t \le h_i^{min} \\ 0 & \text{otherwise} \end{cases} \tag{A11}$$

A3. Trace Length Distribution of Singly Censored Fractures

[48] From the assumptions of spatial randomness, the integrals representing censoring by the upper and lower edges of the window are equal, and so it is sufficient to consider censoring by either edge. For completeness, both approaches are developed here.

[49] A fracture is censored by the lower edge when

$$\begin{gathered}\psi + \lambda \le h_i(\xi) \\ \psi < 0 \\ 0 \le \xi \le w_i\end{gathered} \tag{A12}$$

and then the trace length is $\psi + \lambda$ (equation (A1c)). Figure A3 shows a finite part of the infinite (in the negative ψ direction) region defined by these inequalities and $t_0 \le \psi + \lambda < t$. Thus $I_i^1(\tau)$ and $J_i^1(\tau)$ are given by

$$I_i^1(t) - I_i^1\left(h_i^{min}\right) = \begin{cases} 2\int_{-\infty}^{0} \int_{h_i^{min}-\psi}^{t-\psi} \int_0^{h_i^{-1}(\lambda+\psi)} f(\lambda) d\xi d\lambda d\psi & h_i^{min} < t \le h_i^{max} \\ 0 & \text{otherwise} \end{cases} \tag{A13}$$

$$J_i^1(t) - J_i^1(t_0) = \begin{cases} 2\int_{-\infty}^{0} \int_{t_0-\psi}^{t-\psi} \int_0^{w_i} f(\lambda) d\xi d\lambda d\psi & t_0 \le t \le h_i^{min} \\ 0 & \text{otherwise} \end{cases} \tag{A14}$$

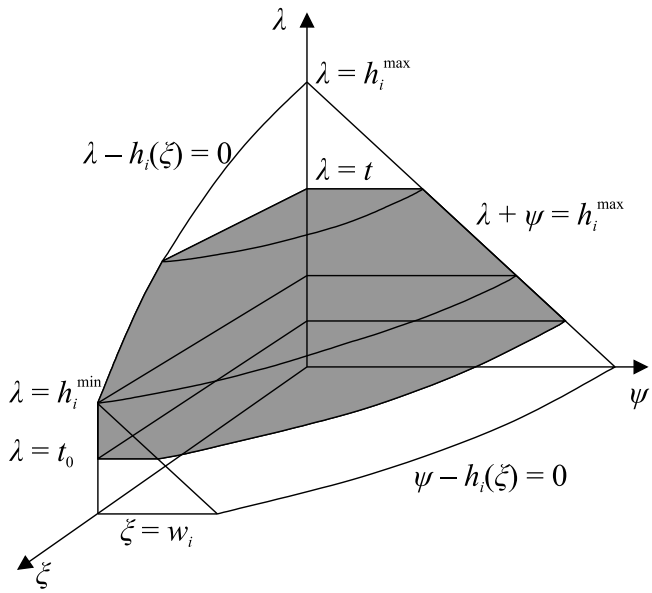

Figure A2. Region of integration for uncensored traces.

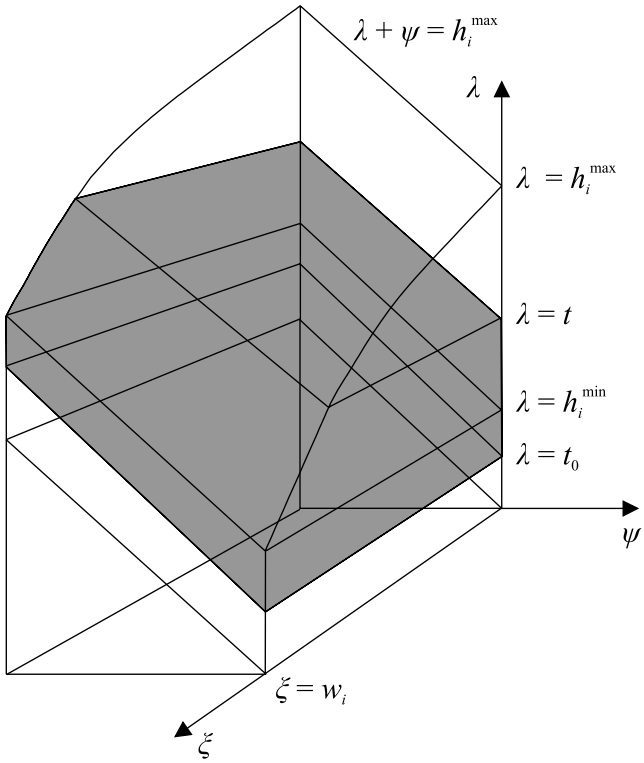

Figure A3. Region of integration for traces censored by the lower edge of the window.

[50] A fracture is censored by the upper edge when

$$\psi + \lambda > h_i(\xi)$$
$$\psi \geq 0 \qquad \text{(A15)}$$
$$0 \leq \xi \leq w_i$$

and then the trace length is $h_i(\xi) - \lambda$ (equation (A1b)). Figure A4 shows a finite part of the infinite region defined by these inequalities and $t_0 \leq \psi + \lambda < t$. Thus $I_i^1(\tau)$ and $J_i^1(\tau)$ are given by

$$I_i^1(t) - I_i^1\left(h_i^{\min}\right) = 2\int_0^{w_i}\int_0^{h_i(\xi)-h_i^{\min}}\int_{h_i(\xi)-\psi}^{\infty} f(\lambda)d\lambda d\psi d\xi - 2\int_0^{h_i^{-1}(t)}\int_0^{h_i(\xi)-t}\int_{h_i(\xi)-\psi}^{\infty} f(\lambda)d\lambda d\psi d\xi \qquad h_i^{\min} < t \leq h_i^{\max} \qquad \text{(A16a)}$$

$$I_i^1(t) - I_i^1\left(h_i^{\min}\right) = 0 \qquad \text{otherwise} \qquad \text{(A16b)}$$

$$J_i^1(t) - J_i^1(t_0) = 2\int_0^{w_i}\int_{h_i(\xi)-t}^{h_i(\xi)-t_0}\int_{h_i(\xi)-\psi}^{\infty} f(\lambda)d\lambda d\psi d\xi \qquad t_0 \leq t \leq h_i^{\min} \qquad \text{(A17a)}$$

$$J_i^1(t) - J_i^1(t_0) = 0 \qquad \text{otherwise} \qquad \text{(A17b)}$$

It is perhaps worth noting here that for evaluating the integrals in equation (A17) in the case of the finite power law, the upper limit of the inner integral must be l_m, the upper cutoff value.

A4. Trace Length Distribution of Doubly Censored Fractures

[51] A fracture is doubly censored when the following inequalities are satisfied:

$$\psi + \lambda > h_i(\xi)$$
$$\psi < 0 \qquad \text{(A18)}$$
$$0 \leq \xi \leq w_i$$

in which case the trace length is $h_i(\xi)$ (equation (A1d)). The first two inequalities can be combined to give limits on ψ and λ:

$$h_i(\xi) - \lambda < \psi < 0$$
$$h_i(\xi) < \lambda \qquad \text{(A19)}$$

When h_i is strictly monotonic, the requirement of the cdf that the trace length $h_i(\xi) < t$, together with the third inequality, can be combined to give that

$$h_i^{-1}(t) < \xi \leq w_i \qquad \text{(A20)}$$

Thus $I_i^2(\tau)$ is defined by

$$I_i^2(t) - I_i^2\left(h_i^{\min}\right) = \int_{h_i^{-1}(t)}^{w_i}\int_{h_i(\xi)}^{\infty}\int_{h_i(\xi)-\lambda}^{0} f(\lambda)d\psi d\lambda d\xi \qquad h_i^{\min} < t \leq h_i^{\max} \qquad \text{(A21a)}$$

$$I_i^2(t) - I_i^2\left(h_i^{\min}\right) = 0 \qquad \text{otherwise} \qquad \text{(A21b)}$$

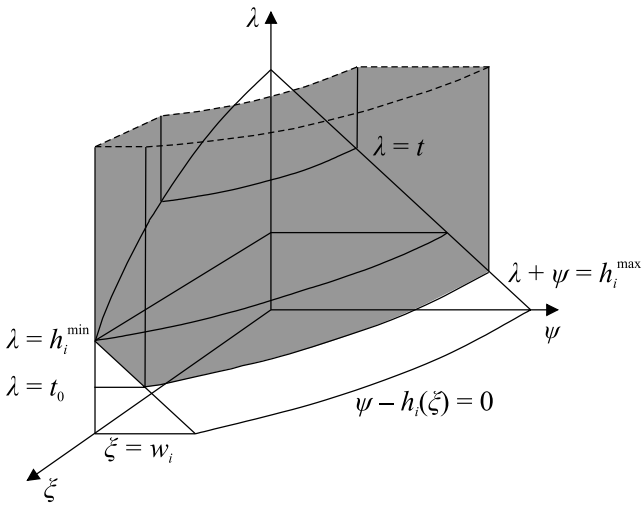

Figure A4. Region of integration for traces censored by the upper edge of the window.

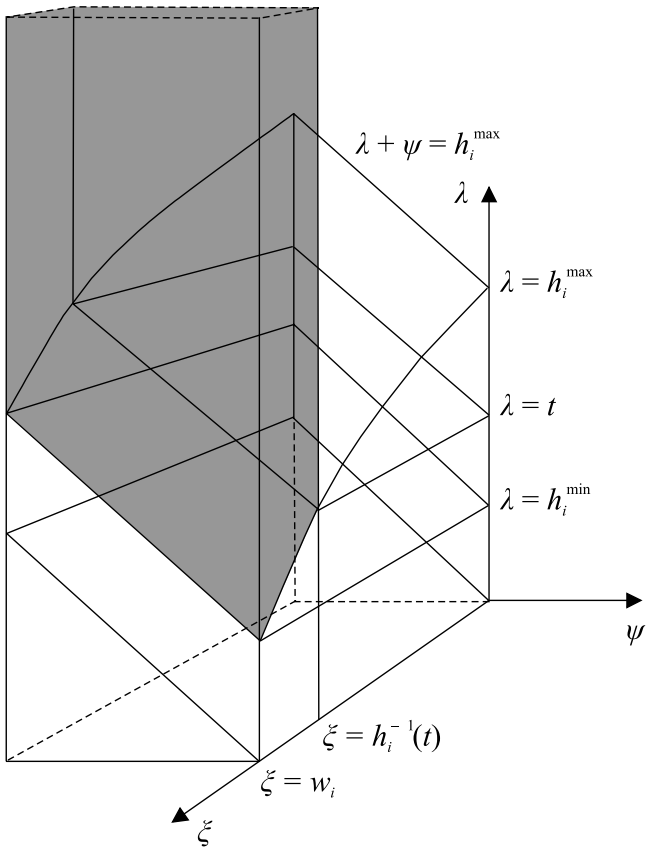

Figure A5. Region of integration for doubly censored traces.

On the other hand, when h_i is constant, the inequalities defining the region of integration are independent of t, and $I_i^2(t) - I_i^2(h_i^{\min})$ is replaced by a constant, I_i^C, defined by

$$I_i^C = \int_0^{w_i} \int_{h_i^{\min}}^{\infty} \int_{h_i^{\min}-\lambda}^{0} f(\lambda) d\psi d\lambda d\xi \qquad \text{(A22)}$$

For doubly censored traces the region below the plane, $\lambda = h_i^{\min}$, is degenerate (Figure A5), and so, to maintain a unified notation, $J_i^2(\tau)$ is defined to be identically equal to zero.

A5. Summary

[52] Since $G_i^j(t)$ is defined by

$$G_i^j(t) = \iiint_{t_0 \le T_i^j < t} f(\lambda) \mathbf{ds} \qquad \text{(A23)}$$

the results from sections A2 to A4 can be summarized in terms of an expanded definition of $G_i^j(t)$, namely,

$$G_i^j(t) = \begin{cases} 0 & t < t_0 \\ J_i^j(t) - J_i^j(t_0) & t_0 \le t \le h_i^{\min} \\ I_i^j(t) - I_i^j\left(h_i^{\min}\right) + J_i^j\left(h_i^{\min}\right) - J_i^j(t_0) & h_i^{\min} < t \le h_i^{\max} \end{cases} \qquad \text{(A24)}$$

equations (A22) and (A24) have been evaluated for three underlying trace length distributions in windows whose heights vary uniformly (Figures 3, 4, and 5). In this case, the function $h_i(\xi)$ is given by

$$h_i(\xi) = h_i^{\max} - \frac{h_i^{\max} - h_i^{\min}}{w_i} \xi \qquad \text{(A25)}$$

[53] **Acknowledgments.** I would like to thank Noelle Odling and an anonymous reviewer for their helpful comments on the manuscript. This work has been funded impart through EU project, ALIANCE, EVK1-CT-2001-00091.

References

Berkowitz, B. (2002), Characterizing flow and transport in fractured geological media: A review, *Adv. Water Resour.*, *25*, 861–884.

Bonnet, E., O. Bour, N. E. Odling, P. Davy, I. Main, P. Cowie, and B. Berkowitz (2001), Scaling of fracture systems in geological media, *Rev. Geophys.*, *39*, 347–383.

Bour, O., and P. Davy (1999), Clustering and size distributions of fault patterns: Theory and measurements, *Geophys. Res. Lett.*, *26*(13), 2001–2004.

Clark, R. M., S. J. D. Cox, and G. M. Laslett (1999), Generalizations of power law distributions applicable to sampled fault-trace lengths: Model choice, parameter estimation and caveats, *Geophys. J. Int.*, *136*, 357–372.

Harris, S. D., E. McAllister, R. J. Knight, and N. E. Odling (2003), Predicting the three-dimensional population characteristics of fault zones: A study using stochastic models, *J. Struct. Geol.*, *25*, 1281–1299.

Jing, L. (2003), A review of techniques, advances and outstanding issues in numerical modelling for rock mechanics and rock engineering, *Int. J. Rock Mech. Min. Sci.*, *40*, 283–353.

Kulatilake, P. H. S. W., and T. H. Wu (1984), Estimation of mean trace length of discontinuities, *Rock Mech. Rock Eng.*, *17*, 215–232.

Laslett, G. M. (1982a), The survival curve under monotone density constraints with applications to two-dimensional line segment processes, *Biometrika*, *69*(1), 153–160.

Laslett, G. M. (1982b), Censoring and edge effects in areal and line transect sampling of rock joint traces, *Math. Geol.*, *14*, 125–140.

Lindsay, R. W., and D. A. Rothrock (1995), Arctic sea ice leads from advanced very high resolution radiometer images, *J. Geophys. Res.*, *100*(C3), 4533–4544.

Lloyd, J. W., R. Greswell, G. M. Williams, R. S. Ward, R. Mackay, and M. S. Riley (1996), An integrated study of controls on solute transport in the Lincolnshire Limestone, *Q. J. Eng. Geol.*, *29*, 321–339.

Odling, N. E. (1997), Scaling and connectivity of joint systems in sandstones from western Norway, *J. Struct. Geol.*, *19*, 1257–1271.

Pahl, P. J. (1981), Estimating the mean length of discontinuity traces, *Int. J. Rock Mech. Min. Sci. Geomech. Abstr.*, *18*, 221–228.

Pascal, C., J. Angelier, M.-C. Cacas, and P. L. Hancock (1997), Distribution of joints: Probabilistic modelling and case study near Cardiff (Wales, U.K.), *J. Struct. Geol.*, *19*, 1273–1284.

Pickering, G., J. M. Bull, and D. J. Sanderson (1995), Sampling power law distributions, *Tectonophysics*, *248*, 1–20.

Riley, M. S. (2004), An algorithm for generating rock fracture patterns: Mathematical analysis, *Math. Geol.*, *36*(6), 683–702.

Song, J.-J., and C.-I. Lee (2001), Estimation of joint length distribution using window sampling, *Int. J. Rock Mech. Min. Sci.*, *38*(4), 519–528.

Visser, C. A., and A. G. Chessa (2000), A new method for estimating lengths for partially exposed features, *Math. Geol.*, *32*(1), 109–126.

White, C. D., and B. J. Willis (2000), A method to estimate length distributions from outcrop data, *Math. Geol.*, *32*(4), 389–418.

Zhang, L., and H. H. Einstein (1998), Estimating the mean trace length of rock discontinuities, *Rock Mech. Rock Eng.*, *31*(4), 217–235.

M. S. Riley, Hydrogeology Research Group, Earth Sciences, School of Geography, Earth and Environmental Sciences, University of Birmingham, Edgbaston, Birmingham B15 2TT, UK. (m.riley@bham.ac.uk)